J. Fluid Mech. (1976), *vol.* 78, *part* 3, *pp.* 561–576
Printed in Great Britain

Fluctuating forces on a rigid circular cylinder in confined flow

By A. RICHTER AND E. NAUDASCHER
Institut für Hydromechanik, Universität Karlsruhe, Germany

(Received 30 March 1976 and in revised form 27 July 1976)

The fluctuating lift and drag acting on a long, rigidly supported circular cylinder placed symmetrically in a narrow rectangular duct were investigated for various blockage percentages over a wide range of Reynolds numbers around the critical value. The data obtained permit a full assessment of the effect of confinement on the mean-drag coefficient, the root-mean-square values of both the drag and the lift fluctuations, the Strouhal number of the dominant vortex shedding, and the Reynolds number marking transition from laminar to turbulent flow separation. Besides experimental information on a subject on which little is known so far, the paper provides a basis for the deduction of better correction procedures concerning the effects of blockage.

1. Introduction

In many engineering problems involving flow around a cylinder, the flow field is contained between parallel walls. It is thus of practical interest to know the influence of confinement on the flow and the flow-induced forces. Moreover, such information is essential to ensure the proper transfer of results from a laboratory study on a cylindrical structure within the confines of a wind or water tunnel to a prototype situation where different confinement conditions are apt to prevail. Information on confinement, or blockage effects is particularly scarce for rounded cylinders over the critical Reynolds-number range in which transition from laminar to turbulent flow separation takes place. In the present paper, experimental results are reported for confined flows around circular cylinders which include that range.

It is difficult to estimate the effects of confining walls on the flow past a cylinder on the basis of previous investigations for a number of reasons. In many reports the magnitude of the confinement ratio is not given, very likely because its significance was not appreciated. In others, there is a lack of information on experimental details that may have an appreciable effect, particularly on flow-induced forces, viz. the turbulence of the approaching stream, the surface roughness of the cylinders, the length-to-diameter (i.e. aspect) ratio of the cylinder, the boundary conditions near the cylinder ends, the elasticity of the cylinder and its supporting system, possible gaps and supporting wires along its span, etc. In a number of studies (e.g. Toebes 1971; Modi & El-Sherbiny 1973), changes in the confinement ratio involved simultaneously changes in the

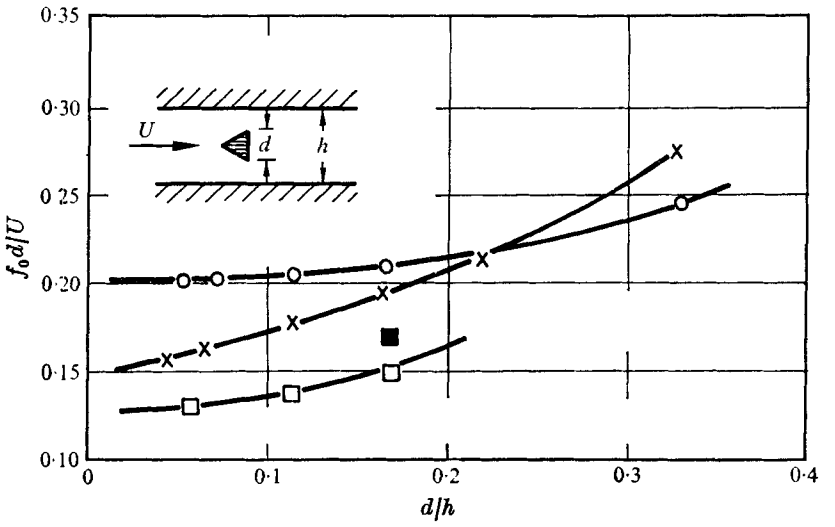

FIGURE 1. Strouhal number $f_0 d/U$ as a function of the confinement ratio d/h for various bluff bodies according to Shaw (1971*b*). $10^3 < Ud/\nu < 10^4$. ×, flat plate; ○, circular cylinder; ■, square cylinder, slightly rounded; □, square cylinder, sharp edged.

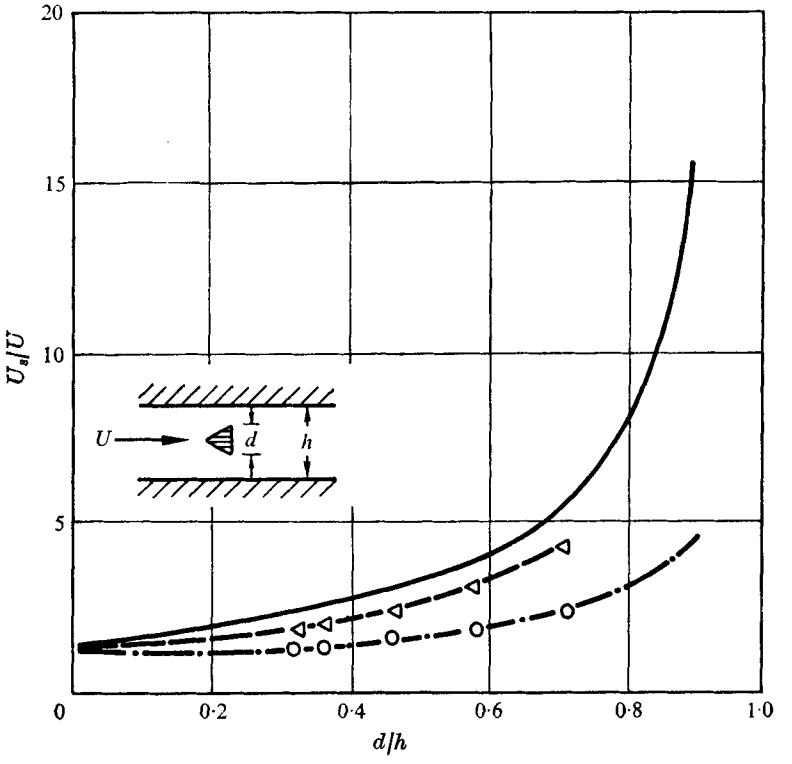

FIGURE 2. Ratio U_s/U of separation velocity to approach-flow velocity as a function of the confinement ratio d/h for various bluff bodies. $10^3 < Ud/\nu < 10^4$. ——, flat plate (Shaw 1971*a*); ◁— —◁, 90 ° wedge (Chen 1967); ○, circular cylinder (Tozkas 1965); —·—, circular cylinder, potential-flow theory (Landweber 1942).

length-to-diameter ratio, so that the effect of the former cannot be discerned independently of the latter. In order to avoid similar uncertainties in the present study, great care was taken to define clearly the experimental conditions and the testing programme.

Before proceeding with the presentation of the results it may be helpful to recall that the effect of flow confinement, or blockage, can be quite different for different forms of the cylinder cross-section. In particular, one has to distinguish between sharp-edged cylindrical bodies (to the limit of a flat plate) with fixed lines of separation, and rounded bodies on which the lines of separation are movable. For example, as shown in figure 1, the variation of Strouhal number $f_0 d/U$ with confinement ratio d/h (where f_0 is the dominant frequency of vortex shedding as obtained from visual observations, U is the average approach velocity and the other symbols are defined in figure 1) is clearly more pronounced for the sharp-edged bodies than for the circular cylinder within the range of Reynolds numbers tested. Moreover, by rounding the corners of a square cylinder only slightly, Shaw (1971*b*) obtained a 12 % increase in Strouhal number. Similar observations apply to the ratio U_s/U, where the separation velocity U_s is defined as the velocity between the wake region and the adjacent walls at a downstream location where the wake width becomes a maximum. Figure 2 shows also that the variation of this parameter with d/h is more pronounced for the sharp-edged forms. Since an increase in the value of U_s/U corresponds to a decrease in base pressure and, hence, to an increase in drag, figure 2 is indicative of the effect of confinement on the drag coefficient.

In the light of the foregoing discussion it becomes evident that none of the currently available correction methods for blockage effect can unreservedly be applied to rounded bodies. The reason is that all of them are based on the assumption of a constant base pressure distribution, and this holds true only for sharp-edged bodies. The well-known method proposed by Glauert (1933), for example, is derived from a potential-flow model and does not allow for a possible shifting of the separation lines. Thus it applies to sharp-edged bodies alone. Indeed, for a circular cylinder, agreement with experimental results could be obtained when the blockage ratio d/h did not exceed about $\frac{1}{4}$, and when the Reynolds number remained below the critical range (Richter 1973). Another much-used correction method is that by Maskell (1963) which is based on a momentum balance of flow outside the wake. Again, the method is only applicable to sharp-edged bodies because it involves the simplifying assumption of a constant base pressure. Any modification of this method for the purpose of making it applicable to circular cylinders, or the development of a new method for this purpose clearly requires a dependable set of experimental data on the effect of confinement on the drag of circular cylinders over a wide, transcritical range of Reynolds numbers. It is this information which is provided here.

2. Experimental arrangement and instrumentation

The tests were undertaken in a specially constructed high-pressure water tunnel 350 cm long featuring a rectangular cross-section with a constant width

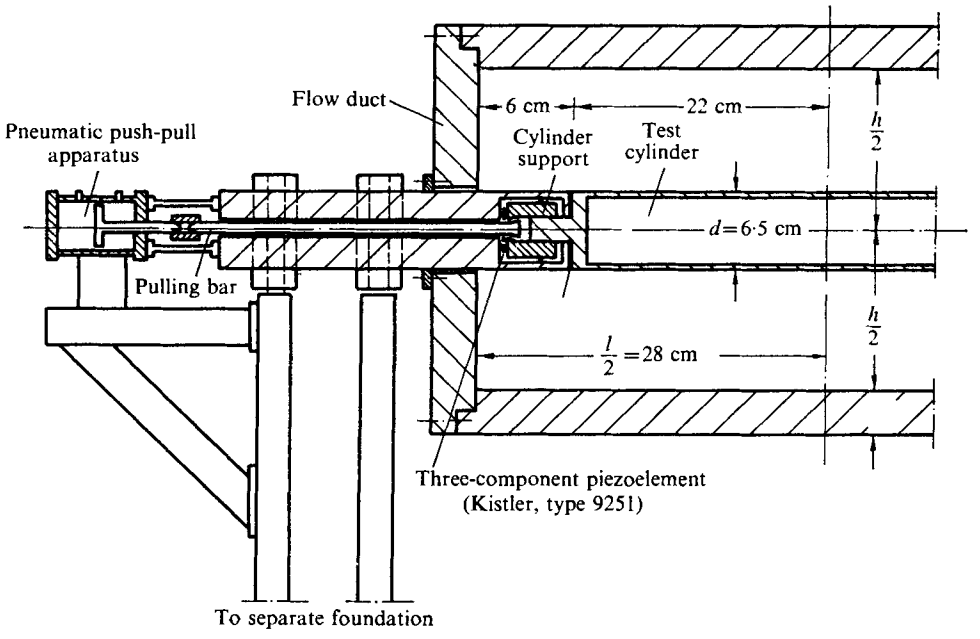

FIGURE 3. Sketch of cylinder support and measurement system.

of 56 cm and step-wise variable height h, 13 cm $\leqslant h \leqslant$ 39 cm. The test section was connected to the upstream supply reservoir of the tunnel assembly by a series of interchangeable, well-rounded contracting sections.

All measurements were performed on the same circular cylinder, which had diameter d = 6·5 cm and length between the tunnel walls l = 56 cm. The reuslting aspect ratio of the cylinder of 8·6 was considered large enough to ensure that the measurements would be representative of an infinitely long cylinder. The test piece was installed symmetrically in the cross-section of the test section, 50 cm downstream from its entrance. To minimize side-wall effects, the instrumented centre part of the cylinder was supported by concentric projecting dummy sections about 6 cm long (figure 3). The distribution of the approach velocity was uniform over 90 % of the cross-sectional area to within $\pm$ 1 % of the average value U; i.e. owing to the short length of flow establishment the effect of the boundary layers developing on the tunnel walls was negligible. The turbulence level u'/U of the approach flow was about 0·5 % $\pm$ 0·1 % throughout the investigated Reynolds-number range $2 \times 10^4 < Ud/\nu < 4 \times 10^5$.

The relative roughness k/d of the polished stainless-steel cylinder was about 0·0008, i.e. small enough according to Teverovskii (1968) not to cause disturbances in the flow. Gaps between the instrumented and the supporting parts of the circular cylinder were filled with an elastic compound and carefully smoothed. The natural frequency of the test cylinder had a value of 12–13 times the dominant frequency of vortex-shedding; moreover, the dynamic system was sufficiently constrained so that displacements of the cylinder did not exceed 0·0003d. Hence, it is safe to assume that the test cylinder behaved like a rigid

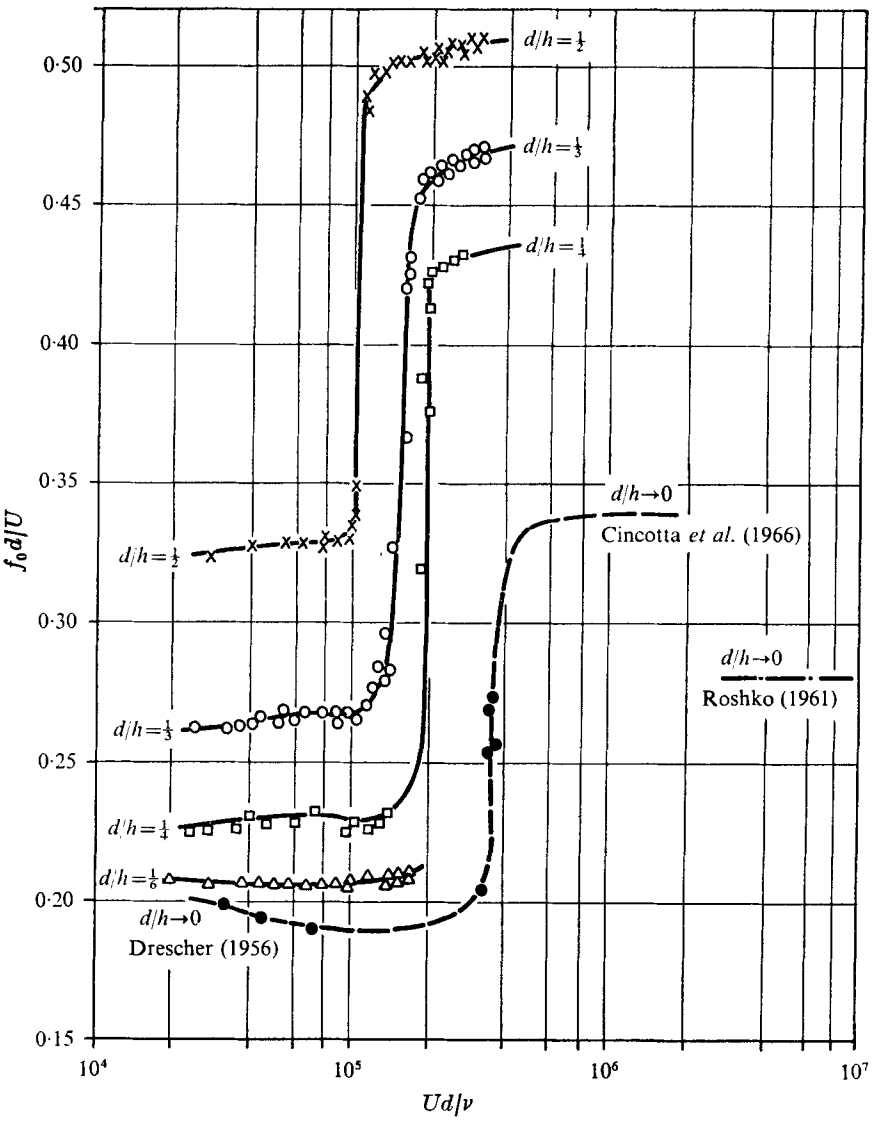

FIGURE 4. Strouhal number *vs.* Reynolds number for various confinement ratios.

one with regard to the flow-induced forces. In view of the required rigidity, piezoelectric-component force transducers were found to be best suited to measure the fluctuating lift and drag. Since force measurement with these transducers is only possible dynamically, during a short period following quasi-static loading, the cylinder supports were simultaneously pressed against the piezo-elements by means of a pneumatic push–pull apparatus before each measurement. When the supports were released, they were held in place by suitable elastic packing. With this arrangement it was possible to measure the mean, the root-mean-square, and the spectra of the fluctuating flow-induced forces. The spectra were determined on-line using a Hewlett Packard Fourier

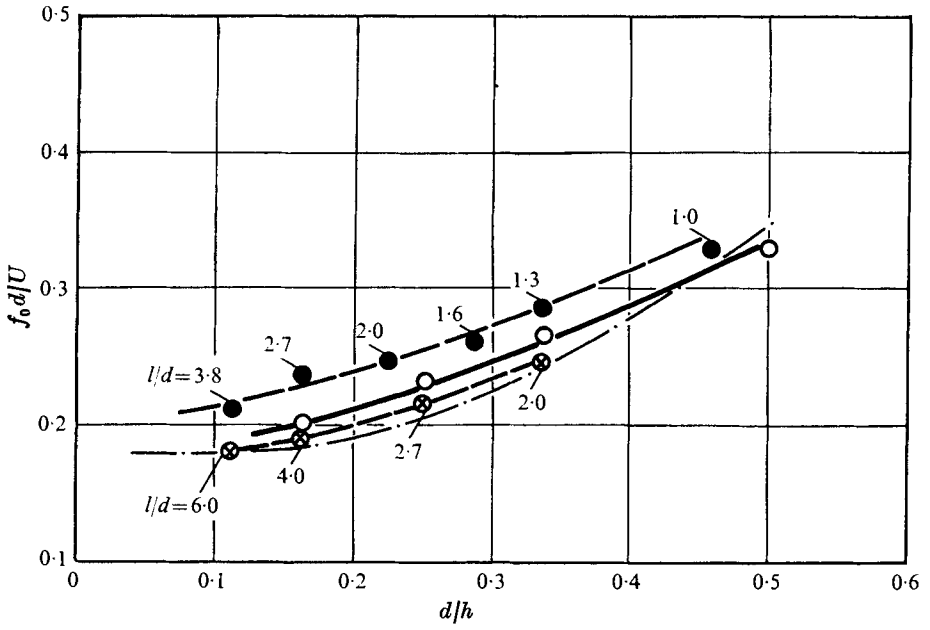

FIGURE 5. Strouhal number as a function of flow confinement in the subcritical Reynolds-number range: $10^4 < Ud/\nu < 10^5$. ⊗——⊗, Shaw (1971); ●——●, Toebes (1971); ○——○, present results; —·—, free-streamline theory.

Analyser, System 5450/5452A. Further details of the method of measurement have been reported by Richter & Stefan (1973).

3. Presentation and discussion of results

3.1. *Strouhal number*

The dominant frequency of vortex shedding from a cylinder is generally described in terms of the Strouhal number $f_0 d/U$, where f_0 corresponds to the peak in the lift spectrum. The present experimental results, evaluated in this way for various values of the confinement ratio, are compared in figure 4 with the findings from experiments with negligible confinement ($h/d \to 0$) of Drescher (1956), Cincotta, Jones & Walker (1966) and Roshko (1961). As can be seen from this figure, increasing flow confinement produces a distinct increase in Strouhal number.

A comparison of the present measurements with those by Shaw (1971) and Toebes (1971) is shown in figure 5 for a subcritical range of Reynolds numbers. In addition, a relationship derived by Roshko (1954) from free-streamline theory, viz.

$$f_0 d/U = 0{\cdot}56\ (d/b^*)\ U_s/U, \tag{1}$$

is presented in the figure. In plotting this relation, use was made of the results of Rosenhead & Schwabe (1930) on the longitudinal spacing of consecutive vortices b^* and Landweber's (1942) prediction of the separation velocity U_s. There is reasonable agreement between Roshko's equation and the experiment-

ally determined Strouhal number of the present study. With regard to the data of Shaw and Toebes, one has to keep in mind that variations in cylinder aspect ratio l/d, as well as end effects and turbulence in approaching flow may have played a role in both cases. Furthermore, Shaw deduced f_0 from visual observations with cylinders of different diameters placed into an open channel, and Toebes evaluated f_0 from spectra using cylinders of various sizes that were instrumented from wall to wall in a rectangular duct of fixed cross-section dimensions. In contrast, l/d was kept constant between the tunnel walls at 8·6 in the present study, and end effects were minimized by instrumenting only a midsection of the cylinder of $6{\cdot}8d$ length. Indeed, since l/d was smaller than 3·8 in all of Toebes's tests, one must suspect from the findings of Graham (1969) that the vortex shedding in his case was synchronized and, hence, distinctly different from that occurring on an infinitely long cylinder.

To the best of the authors' knowledge, there is so far no information available on the effect of confinement on flow characteristics within the critical Reynolds-number range. Because of the contraction of the wake which accompanies the downstream shift of the separation lines with transition from a laminar to a turbulent boundary layer, a rise in Strouhal number is to be expected in this range (Bearman 1969). It is interesting to note from figure 4 how abrupt, irrespective of confinement, this rise actually is despite the fact that changes in drag and lift characteristics occur much more gradually. The peaks in the lift spectra were clearly discernible during the experiments even in the transition range, although the bandwidth was somewhat broadened. The sharp rise in Strouhal numbers was explained by Roshko (1961) with the observation that, early in transition, the initial boundary-layer separation is followed by re-attachment enclosing a 'bubble', before the second and final separation. In this way, the location of the separation lines on the cylinder surface is displaced rather suddenly by a substantial distance downstream. Judging from the shape of the curves in figure 4, it stands to reason that a similar type of bubble formation takes place in a confined flow as well. With further increase in Reynolds number to, say, $Ud/\nu > 10^6$, the separation bubble vanishes and the separation lines move upstream, giving rise to a lower frequency of vortex shedding owing to the resulting larger distance between the separated shear layers. The Strouhal number in this supercritical range is therefore lower than in the transition range, which explains the difference in the data of Roshko (1961) and Cincotta *et al.* (1966) shown in figure 4. A similar drop in Strouhal number with an increase in Reynolds number beyond the transitional range may also be expected to occur in confined flow.

It is of interest, finally, to replot the data of figure 4 in terms of the universal Strouhal number $f_0 d^*/U^*$ (and corresponding Reynolds number), defined by Roshko (1954) with the aid of the wake width between the rows of vortices d^* and the velocity along the free streamline delineating the wake U^*; and to compare the result with the value of $f_0 d^*/U^* = 0{\cdot}16$ found by Roshko (1954) for bluff bodies of different cross-sectional forms in unconfined flow, including the circular cylinder in the subcritical range. Thus, using the relation between d^*/d and U_s/U deduced by Roshko (1954) for a circular cylinder, in combination

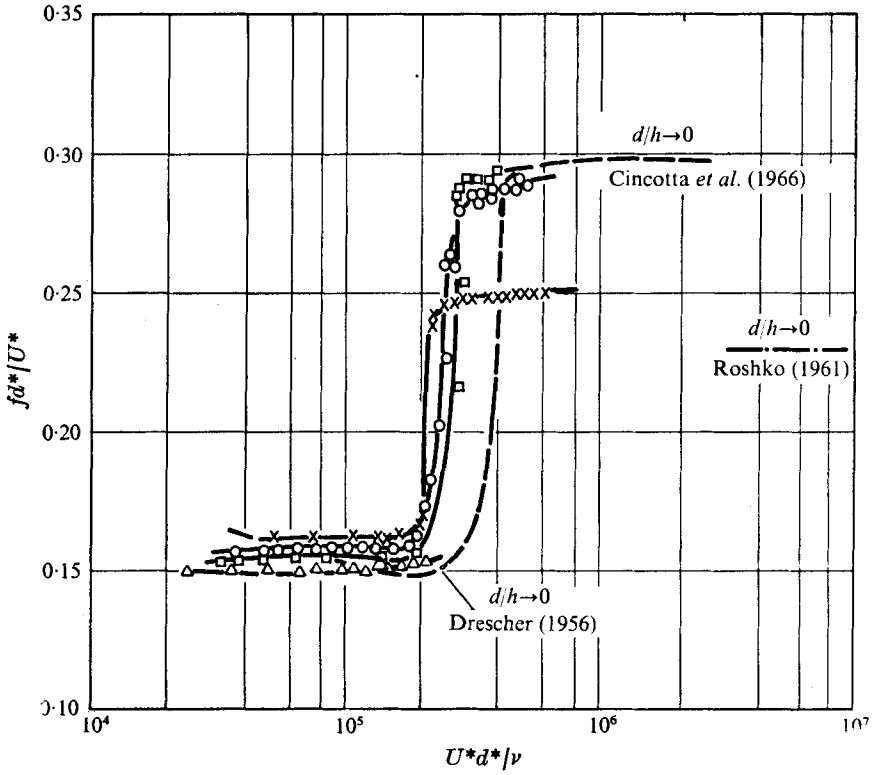

FIGURE 6. 'Universal' Strouhal number *vs.* Reynolds number for various confinement ratios. ×, $d/h = \frac{1}{2}$; ○, $d/h = \frac{1}{3}$; □, $d/h = \frac{1}{4}$; △, $d/h = \frac{1}{6}$.

with the data of figure 2 and the continuity equation $U^*/U = h/(h-d^*)$, one obtains the diagram of figure 6. This shows that, in the subcritical range of Reynolds numbers, the values of $f_0 d^*/U^*$ lie within $\pm 5\,\%$ of the value of 0·16 for all confinement conditions tested. The finding confirms that the concept of a universal Strouhal number can be extended to confined flow past a circular cylinder.

3.2. *Critical Reynolds number*

There are different ways of defining the critical Reynolds number at which laminar conditions in the boundary layer along the cylinder change into turbulent. In view of the sudden rise in Strouhal number, as compared with the more gradual variations in drag and lift characteristics within the transitional range (see figures 7 and 9), the location of the former appears to be the logical choice for this definition.

It is evident from figure 4 that the magnitude of the critical Reynolds number expressed in terms of the approach velocity and cylinder diameter decreases with increasing flow confinement. However, as seen from a comparison with figure 6, most of this decrease can be interpreted as resulting from the use of the velocity U instead of the shear-layer velocity U^*, which is clearly the significant variable concerning boundary-layer transition.

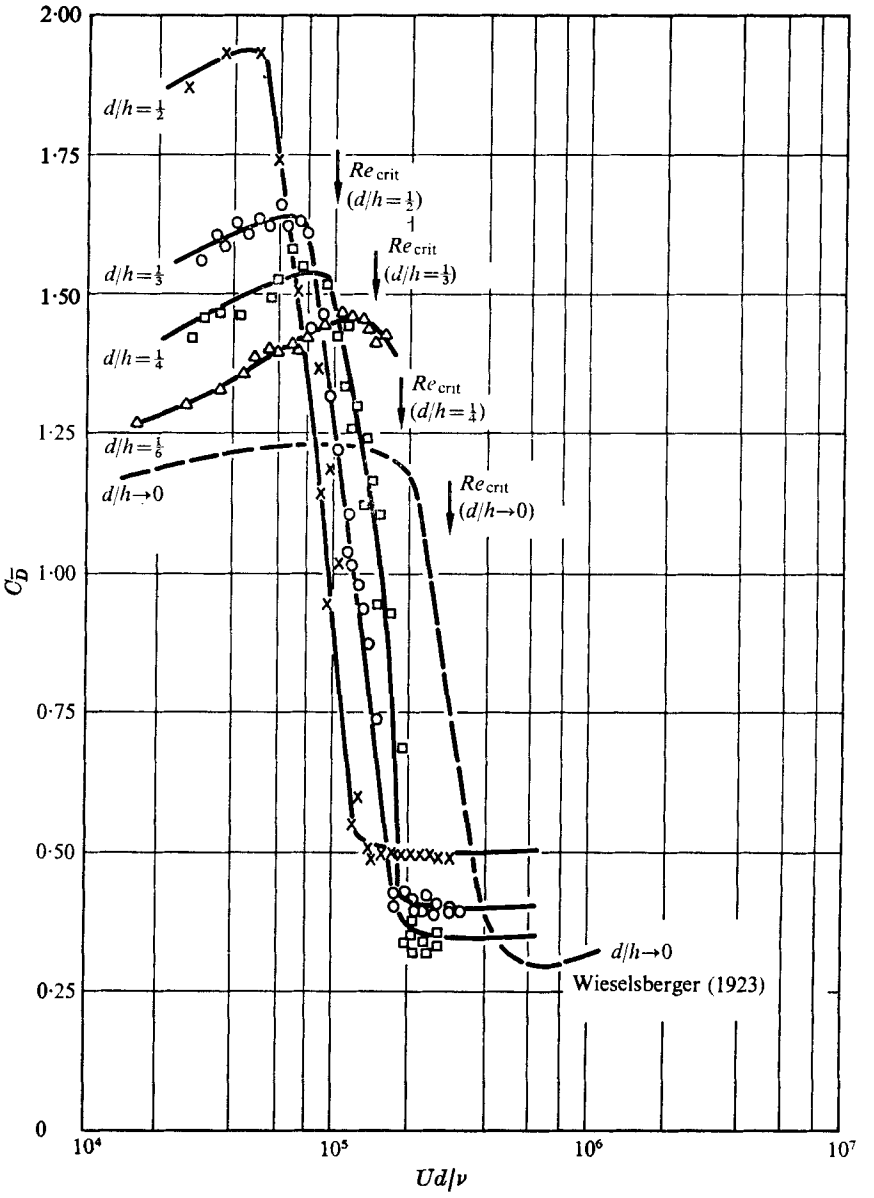

FIGURE 7. Mean-drag coefficient *vs.* Reynolds number for various confinement ratios.

3.3. *Mean drag*

The coefficient of mean drag is defined as

$$C_{\bar{D}} = \bar{D}/l_m d\tfrac{1}{2}\rho U^2, \tag{2}$$

where $\bar{D}$ is the time-mean value of the drag, l_m is the length of the cylinder section over which the flow-induced forces are being measured and ρ is the fluid density. Data on $C_{\bar{D}}$ as a function of the Reynolds number are presented in figure 7, including data of Wieselsberger (1923) for an unconfined circular

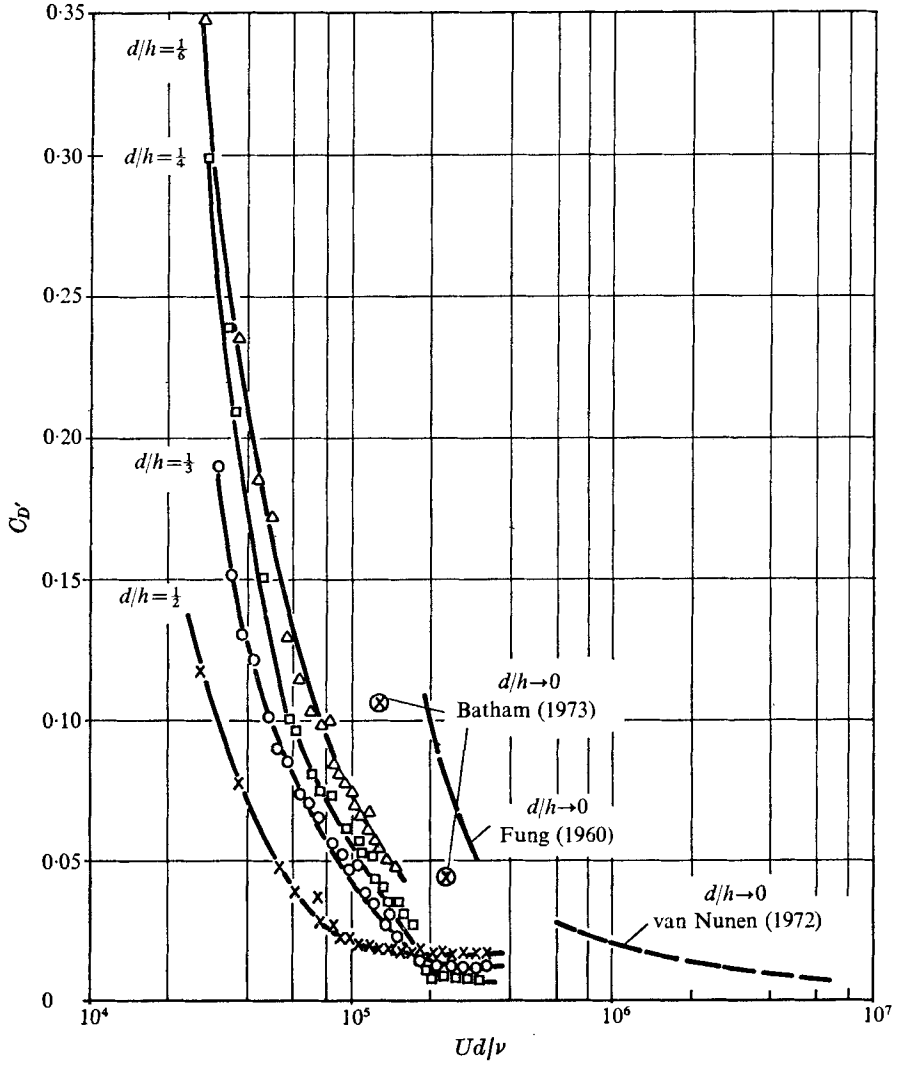

FIGURE 8. Fluctuating-drag coefficient *vs.* Reynolds number for various confinement ratios.

cylinder. The diagram reveals that increasing flow confinement leads to larger values of the mean drag coefficient. The increase is undoubtedly a consequence of the lower base pressures which are brought about by higher separation velocities in confined flow situations (figure 2).

The onset of the characteristic decrease in drag coefficient occurs at Reynolds numbers slightly smaller than the critical value obtained in figure 4. The likely reason for this is discussed below. From figure 7 it can be verified that C_D for the critical Reynolds number as determined from figure 4 is very close to the value 0·8 for all confinement conditions investigated. It is interesting to note that the definition of the critical Reynolds number by Bearman (1968), i.e. the Reynolds number at which C_D reaches 0·8, can thus be extended to confined flow as well.

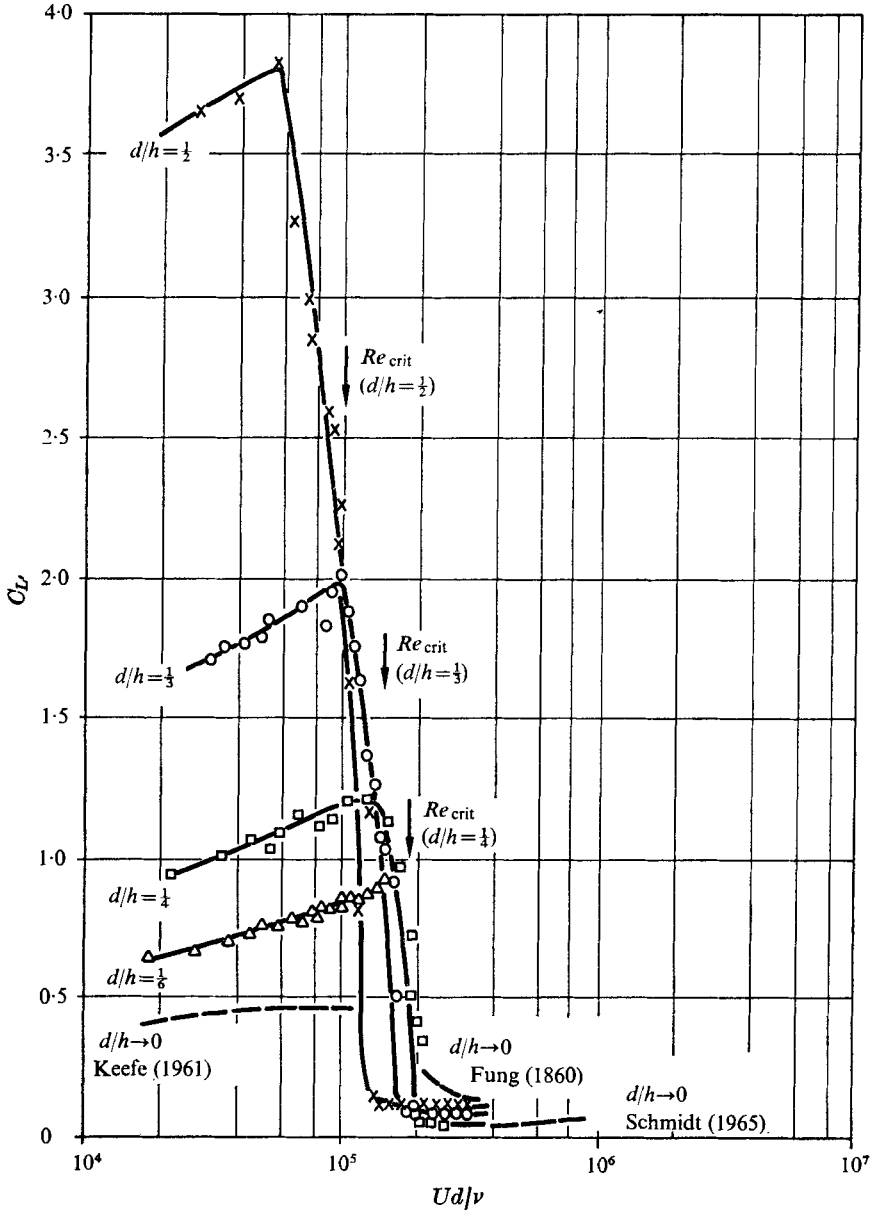

FIGURE 9. Fluctuating-lift coefficient *vs.* Reynolds number for various confinement ratios.

3.4. *Fluctuating drag and lift*

The coefficient of fluctuating drag is defined by the root mean square of the drag fluctuations D' as obtained from an integration of the corresponding frequency spectrum, viz.

$$C_{D'} = \overline{(D'^2)}^{\frac{1}{2}}/l_m d\tfrac{1}{2}\rho U^2. \tag{3}$$

A plot of $C_{D'}$ as a function of Reynolds number is presented in figure 8. The diagram combines present results and data by Fung (1960), van Nunen (1972)

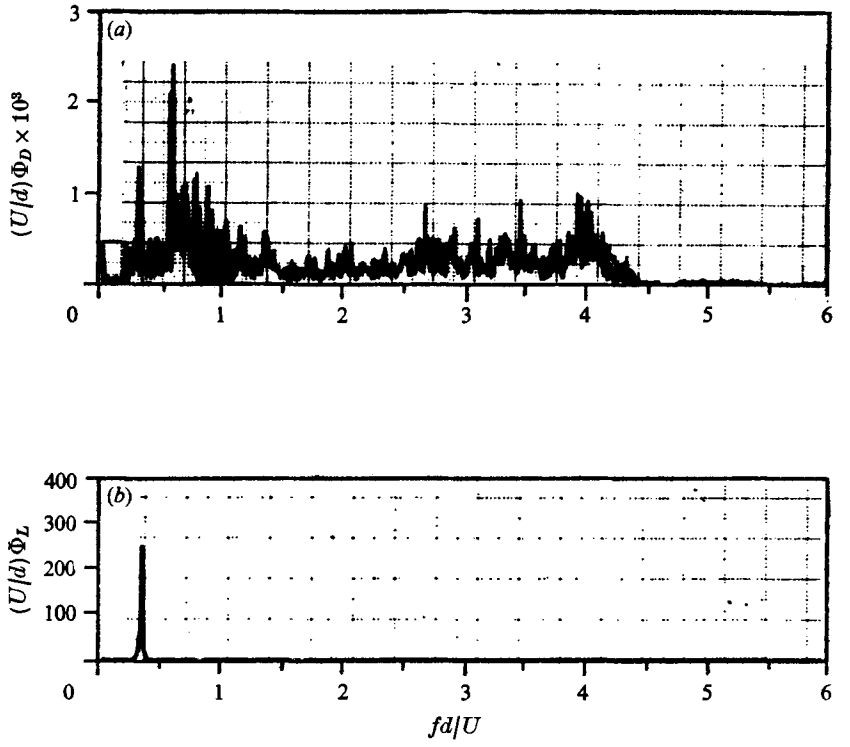

FIGURE 10. Spectra for $Ud/\nu = 3 \times 10^4$ and $d/h = \frac{1}{2}$ of (*a*) the fluctuating drag and (*b*) the fluctuating lift.

and Batham (1973). According to these results, the intensity of fluctuating drag becomes smaller with flow confinement except for the range beyond the critical Reynolds number. Within the entire range of measurement, and for all confinement ratios, $C_{D'}$ decreases monotonically with increasing Reynolds number down to very small values.

The transition from laminar to turbulent flow in the boundary layer on the cylinder, and the corresponding shift of the separation lines in the downstream direction, is clearly a more gradual process than the Strouhal-number diagram (figures 4 or 6) would seem to indicate. A decreasing spanwise correlation accompanying a greater spanwise variation of the time-dependent separation events, and an increasing three-dimensionality of the flow along the span of the cylinder prior to the general downstream shift of the lines of separation may be part of the explanation for this gradual decrease in the drag coefficient (as well as for the decrease in the lift coefficient depicted in figure 9). Since D' is much more sensitive to this three-dimensionality than either $\overline{D}$ or L' (as is demonstrated by the extremely broad spectral distribution of D' as compared with that of L' in figure 10), it is reasonable that $C_{D'}$ should start to become affected by it at lower Reynolds numbers than either $C_{\overline{D}}$ or $C_{L'}$. Of course, the spectrum of the fluctuating drag is also influenced by the turbulence in the cylinder wake.

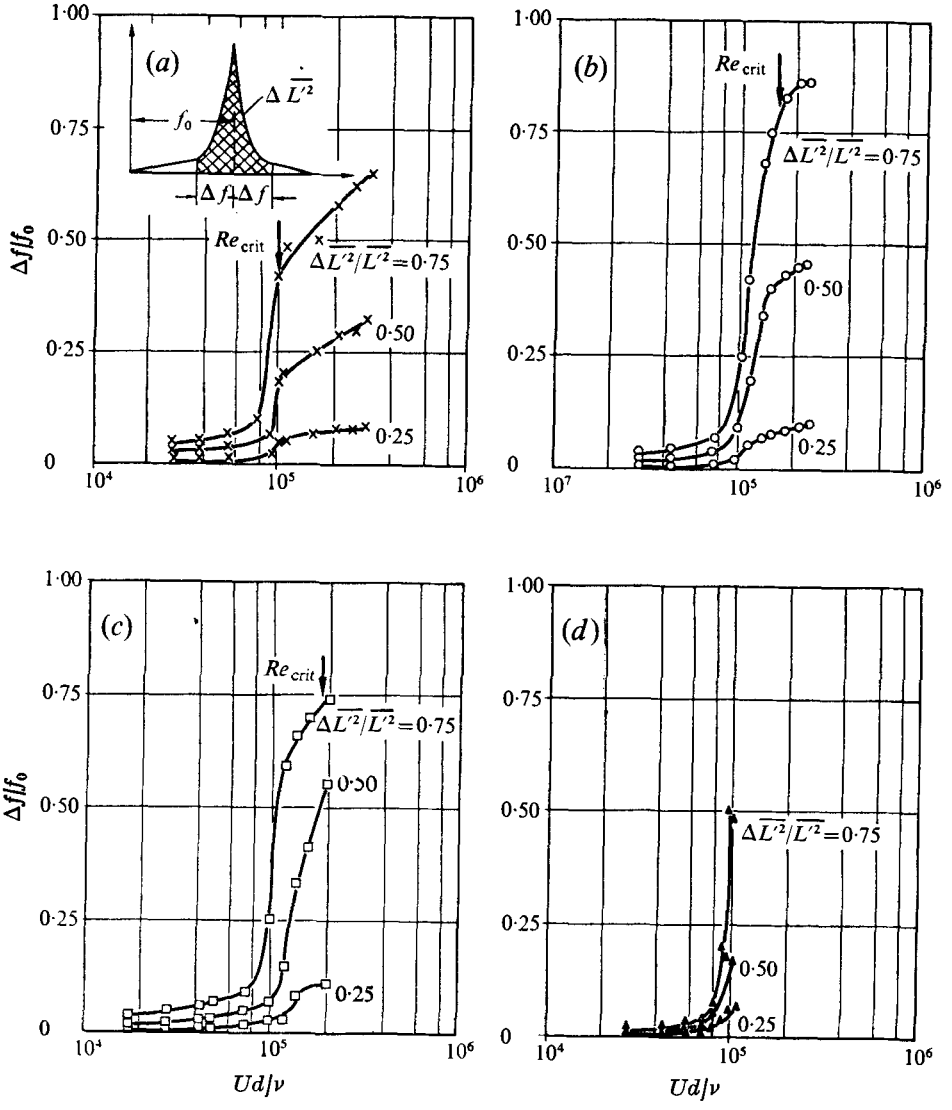

FIGURE 11. Characteristic bandwidth of lift fluctuations *vs.* Reynolds number for different confinement ratios. (*a*) $d/h = \frac{1}{2}$. (*b*) $d/h = \frac{1}{3}$. (*c*) $d/h = \frac{1}{4}$. (*d*) $d/h = \frac{1}{6}$.

The variation of the coefficient of fluctuating lift, i.e.

$$C_{L'} = (\overline{L'^2})^{\frac{1}{2}}/l_m d\tfrac{1}{2}\rho U^2, \tag{4}$$

with Reynolds number and confinement ratio is depicted in figure 9. The present findings are complemented by data of Fung (1960), Keefe (1961), and Schmidt (1965). All of the curves shown first exhibit a gradual rise with increasing Reynolds number, and then fall sharply just before the critical Reynolds number is reached. It seems worthwhile noting that $C_{L'}$ attains values in excess of the mean-drag coefficient C_D as confinement is increased.

An example of the spectral distribution of the lift fluctuations in non-dimensional form is shown in figure 10(*b*). In this, $\phi_L(f)$ is the spectral-density function defined such that $\overline{L'^2} = \int_0^\infty \overline{L'^2}\,\phi_L(f)\,df$, and f is the frequency. In order to show graphically the dependence of the lift spectra on Reynolds number and confinement ratio, these spectra were further processed as illustrated in the definition sketch inserted in figure 11. The four main diagrams in this figure (each for a different value of confinement) show, as a function of Reynolds number, those frequency bandwidths Δf in relation to the dominant frequency f_0 that correspond to given values of $\Delta\overline{L'^2}/\overline{L'^2}$ (i.e. 0·25, 0·50, and 0·75), where $\Delta\overline{L'^2}$ represents that part of the whole mean-square value of the lift fluctuations $\overline{L'^2}$ which is associated with frequencies f between the limits $(f_0-\Delta f) < f < (f_0+\Delta f)$. The smaller Δf for a given $\Delta\overline{L'^2}/\overline{L'^2}$, of course, the more pronounced is the peak in the spectrum, or the more nearly periodic are the lift fluctuations. One may thus conclude from figure 11 that, for all confinement conditions investigated, the degree of randomness in the lift fluctuations increases consistently as Ud/ν approaches and passes the critical Reynolds number. For the subcritical Reynolds numbers investigated, 75 % of the mean-square lift fluctuations are associated with frequencies lying within a bandwidth of $\pm 0{\cdot}08 f_0$ around the dominant frequency f_0. In that same range, this 75 % bandwidth is seen to decrease consistently with decreasing Reynolds number. A comparable reduction in bandwidth, indicating increasing periodicity, is obtained as the confinement ratio d/h is reduced from $\frac{1}{4}$ to $\frac{1}{6}$. There is no measurable effect for larger confinement.

4. Conclusions

Increasing flow confinement was found to increase the Strouhal number throughout the transcritical range of Reynolds numbers. Near transition, the rise in Strouhal number is very sudden even though the changes in drag and lift characteristics are gradual; it can therefore be conveniently used to define the critical Reynolds number. The observed reduction in critical Reynolds number with growing flow confinement is a consequence of increases in separation and shear-layer velocities. The concept of a universal Strouhal number may be considered confirmed as applying to confined flow conditions as well.

Since higher separation velocities lead to lower base pressures, flow confinement increases the mean drag. The drop in mean-drag coefficient near the critical range becomes more pronounced with larger confinement. With the Reynolds number approaching the critical value, growing three-dimensionality and randomness of the separating flow affect the fluctuating-drag coefficient more than any other characteristic. Whereas flow confinement reduces the magnitude of this coefficient in the subcritical range, the opposite holds true with regard to the coefficient of fluctuating lift. For a confinement ratio $d/h = \frac{1}{2}$, the latter reaches values of up to eight times that for unconfined flow, just before dropping off near the critical Reynolds number. This finding is the more

remarkable as the corresponding spectrum manifests a pronounced peak with 75 % of the mean-square lift fluctuations concentrated within a bandwidth of ± 8 % of the dominant frequency.

The major part of this research was supported by the Deutsche Forschungsgemeinschaft (DFG) under contract number Na 75/5. The authors express their appreciation to Dr Hans J. Leutheusser for critically reviewing the text.

REFERENCES

BATHAM, J. P. 1973 Pressure distributions on circular cylinders at critical Reynolds numbers. *J. Fluid Mech.* **57**, 209–228.

BEARMAN, P. W. 1969 The flow around a circular cylinder in the critical Reynolds number regime. *J. Fluid Mech.* **37**, 577–585.

CHEN, Y.-S. 1967 Effect of confining walls on the periodic wake of 90-degree wedges. Master's thesis, University of Iowa.

CINCOTTA, J. J., JONES, G. W. & WALKER, R. W. 1966 Experimental investigation of wind-induced oscillation effects on cylinders in two-dimensional flow at high Reynolds numbers. *Meeting on Ground Wind Load Problems in Relation to Launch Vehicles, N.A.S.A. Langley Research Center.*

DRESCHER, H. 1956 Messung der auf querangeströmte Zylinder ausgeübten zeitlich veränderten Drücke. *Z. Flugwiss.* **4**, 17–21.

FUNG, Y. C. 1960 Fluctuating lift and drag acting on a cylinder in a flow at supercritical Reynolds numbers. *J. Aero. Sci.* **27**, 801–814.

GLAUERT, H. 1933 Wind tunnel interference on wings, bodies, and airscrew. *Aero. Res. Counc. R. & M.* no. 1566.

GRAHAM, J. M. R. 1969 The effect of end-plates on the two-dimensionality of a vortex wake. *Aero. Quart.*, August, 237–247.

KEEFE, R. T. 1961 An investigation of the fluctuating forces acting on a stationary circular cylinder in a subsonic stream and of the associated sound field. *Univ. Toronto, Inst. Aerophys. Rep.* no. 76.

LANDWEBER, L. 1942 Flow about a pair of adjacent, parallel cylinders normal to a stream. *David W. Taylor Model Basin, Dept. Navy, Rep.* no. 485.

MASKELL, E. C. 1963 Theory of blockage effects on bluff bodies and stalled wings in a closed wind tunnel. *Aero. Res. Counc. R. & M.* no. 3400.

MODI, V. J. & EL-SHERBINY, S. 1973 On the wall confinement effects in industrial aerodynamics studies. *Int. Symp. Vibration Problems in Industry, Keswick, England,* paper 116.

NUNEN, J. W. G. VAN 1972 Steady and unsteady pressure and force measurements on a circular cylinder in a cross flow at high Reynolds numbers. In *Flow-Induced Structural Vibrations* (ed. E. Naudascher). Springer.

RICHTER, A. 1973 Strömungskräfte auf starre Kreiszylinder zwischen paralellen Wänden. Disseration, Universität Karlsruhe.

RICHTER, A. & STEFAN, K. 1973 Anwendung piezoelektrischer Mehrkomponenten-Kraftmesser in der Stromungsmechanik. *Arch. Tech. Messen*, **5**, 131–311.

ROSENHEAD, L. & SCHWABE, M. 1930 An experimental investigation of the flow behind circular cylinders in channels of different breadth. *Proc. Roy. Soc.* A **129**, 115–135.

ROSHKO, A. 1954 On the drag and shedding frequency of two-dimensional bluff bodies. *N.A.C.A. Tech. Note*, no. 3169.

ROSHKO, A. 1961 Experiments on the flow past a circular cylinder at very high Reynolds numbers. *J. Fluid Mech.* **10**, 345–356.

SCHMIDT, L. V. 1965 Measurements of fluctuating air loads on a circular cylinder. *J. Aircraft*, **2**, 49–55.

SHAW, T. L. 1971*a* Effect of side walls on flow past bluff bodies. *J. Hydraul. Div. A.S.C.E.* **97**, 65–79.

SHAW, T. L. 1971*b* Wake dynamics of two-dimensional structures in confined flows. *14th Congr. Int. Ass. Hydraul. Res., Paris*, paper B 6.

TEVEROVSKII, B. M. 1968 Effect of surface roughness on the vibration of a cylinder in hydrodynamic conditions. *Russian Engng J.* **48**, 12, 50–54.

TOEBES, G. H. 1971 The frequency of oscillatory forces acting on bluff cylinders in constricted passages. *14th Cong. Int. Ass. Hydraul. Res., Paris*, paper B 7.

TOZKAS, A. 1965 Effect of confining walls on the periodic wake of cylinders and plates. Master's thesis, University of Iowa.

WIESELSBERGER, G. 1923 Der Widerstand von Zylindern. *Ergebnisse der Aerodynamischen Versuchsanstalt Göttingen*, II. *Lieferung*, pp. 23–28.